Binary Morphological Shape-Based Interpolation Applied to 3-D Tooth Reconstruction

Adrian G. Borş*, *Member, IEEE*, Lefteris Kechagias, and Ioannis Pitas, *Senior Member, IEEE*

***Abstract*—In this paper, we propose an interpolation algorithm using a mathematical morphology morphing approach. The aim of this algorithm is to reconstruct the n-dimensional object from a group of $(n-1)$-dimensional sets representing sections of that object. The morphing transformation modifies pairs of consecutive sets such that they approach in shape and size. The interpolated set is achieved when the two consecutive sets are made idempotent by the morphing transformation. We prove the convergence of the morphological morphing. The entire object is modeled by successively interpolating a certain number of intermediary sets between each two consecutive given sets. We apply the interpolation algorithm for three-dimensional tooth reconstruction.**

***Index Terms*—Mathematical morphology, morphing, shape-based interpolation.**

I. Introduction

In MANY tasks, we have to extract object information from a group of sparse sets. Particularly, in medical applications, parts of human body are represented by an image sequence of parallel slices. These slices can be acquired by magnetic resonance imaging (MRI), computer tomography (CT), or by mechanical slicing and digitization. Most often, the distance between adjacent image elements within a slice is smaller than the distance between adjacent image elements in two neighboring slices. In such situations, it is necessary to interpolate additional slices in order to obtain an accurate description of the object for volume visualization and processing [1]. There are two main categories of interpolation techniques for reconstructing objects from sparse sets: grey-level and shape-based interpolation.

Grey-level interpolation methods employ nearest-neighbor, splines, linear [2], or polynomial interpolation. Other algorithms employ feature matching [3] or homogeneity similarity [4] for determining the direction of interpolation.

Shape-based interpolation algorithms are usually employed on binary images. These interpolation methods consider shape features extracted from the object sets. A distance function from each pixel to the object boundary is considered for interpolation in [5]. In [6], an interpolation–extrapolation algorithm is introduced which has similarities with that from [5]. Other extensions of the algorithm described in [5] are proposed in [7] and [8]. Among six different algorithms, the one based on a chamfer distance and using a modified cubic spline was found to provide the best results in [7]. An interpolation algorithm which uses the elastic matching algorithm, spline theory, and surface consistency is considered in [9]. Shape-based interpolation methods have been shown to outperform other interpolation methods in [10]. A mixed gray-level and shape-based method is used for interpolation in [11]. Each slice is represented as a surface by a "lifting" procedure. The intermediary slices are obtained by interpolating the resulting surfaces and converting the interpolated surface back to an image by a "collapsing" operation.

Mathematical morphology provides a good theoretical framework for shape modeling and interpolation [12], [13]. Erosion and dilation are basic morphologic transformation operations. In [14], each slice is eroded until its number of pixels becomes half of the sum of its initial number of pixels and those of the next slice. Morphing based on a distance transform is used for slice interpolation in [15]. Interpolated sets in [16] are generated from a succession of skeletons derived from the matching of two neighboring set skeletons. The skeleton by influence zone (SKIZ) transform employs dilations of the intersection and of the complementary of the union of two neighboring sets [17].

In this paper, we propose a new binary morphological morphing approach for interpolation. The morphing transforms two neighboring sets by combinations of dilations and erosions. The transformation is iteratively performed in such a way that the resulting sets become more similar to each other with respect to both shape and dimension. We define a distance measure for assessing the difference between the original and the morphed shape. The interpolated set corresponds to the idempotency of the two morphed sets after a certain number of iterations. Idempotency is achieved when the difference of the morphed sets is zero. The morphing transformation is applied repeatedly on the new stack of interpolated sets until an appropriate object shape is achieved. We employ the morphological morphing approach for reconstructing three-dimensional (3-D) teeth from digitized slices.

This paper is organized as follows. Section II describes the morphological morphing transformation and Section III the interpolation algorithm. In Section IV, we provide some experimental results. The conclusions of this study are drawn in Section V.

II. Morphological Morphing

Let us consider that we are provided with two sets representing two shapes, denoted by P and Q, in an n-dimensional

Manuscript received May 7, 1999; revised December 11, 2001. This work was supported in part by GSRT and the European Social Fund under Research Project 99ED 599 (PENED 99). The Associate Editor responsible for coordinating the review of this paper and recommending its publication was M. W. Vannier. *Asterisk indicates corresponding author.*

*A. G. Borş was with the Department of Informatics, University of Thessaloniki, Thessaloniki 540 06, Greece. He is now with the Department of Computer Science, University of York, YO10 5DD York, U.K. (e-mail: adrian.bors@cs.york.ac.uk).

L. Kechagias and I. Pitas are with the Department of Informatics, University of Thessaloniki, Thessaloniki 540 06, Greece.

Publisher Item Identifier S 0278-0062(02)02938-5.

space denoted as E. Shape morphing is a technique for constructing a sequence of sets showing a gradual transition between the two given shapes. In the following, we describe a morphological morphing transformation.

The simplest morphological operations are the dilation and erosion [12]. These operations correspond to the Minkowski set addition and subtraction. The dilation of a set P by using the structuring element B is given by

$$P \oplus B = \bigcup_{b \in B} P_b \tag{1}$$

where $\oplus$ denotes dilation and P_b represents a structuring element centered onto an element of the set P. The erosion of a set P by using the structuring element B is given by

$$P \ominus B = \bigcap_{b \in B} P_b \tag{2}$$

where $\ominus$ denotes erosion. The most commonly used structuring element is the elementary ball of dimension n. The dilation with the elementary ball expands the given set with a uniform layer of elements while the erosion operator takes out such a layer from the given set.

The basic mathematical morphology operations defined above can be used to derive complex processing operations [12], [13]. Let $p' \in P$ and $q \in Q$ be the elements of the sets P and Q. Let w: $p' \longrightarrow p$ be an alignment transform that aligns P with Q, such that we have $\{\exists(p_m, q_m) | p_m \in P, q_m \in Q\}$. The alignment operation is done according to an $(n-1)$-dimensional hyperplane [axis for two-dimensional (2-D) sets] using matching of corresponding features or a centering operation. We define the complement (background) of the set P by $P^c = E - P$. After alignment, each element p_m will have a corresponding element q_m which may be a member of the other set $q_m \in Q$, or may be part of its background $q_m \in Q^c$. In [5], algorithms that use distance transforms for morphing interpolated sets by adding or removing layers of elementary units have been proposed. In [17], the SKIZ was used for set and function interpolation. The interpolated set in [17] is obtained by means of successive dilations of the sets $P \cap Q$ and $E - (P \cup Q)$, until idempotency is achieved. However, such an approach does not correspond to a natural morphing of one set into the other one.

The morphing transformation proposed in this paper ensures a smooth transition from one shape set to the other one by means of several sets whose shapes change gradually. First, our transformation influences the elements located on the boundary of the set P

$$C_P = \{c | c \in P, \exists c_1 \in P^c, c_1 \in \mathcal{N}_B(c)\} \tag{3}$$

where $\mathcal{N}_B(c)$ denotes the neighborhood of the element c, having the same size and shape as the structuring element B. In our morphing operation, the elements of a boundary set C_P are changed differently according to their correspondences on the other given set Q [18], [19]. These changes are defined in terms of mathematical morphology basic operations such as dilations (1) and erosions (2). We can identify three possible correspondence cases for the elements of the two aligned sets. One situation occurs when the border region of one set corresponds to the interior of the other set. In this case, we apply the morphological operation of dilation to the border elements

$$\begin{aligned} \text{If} \quad & p_m \in C_P \wedge q_m \in Q - C_Q \\ \text{then} \quad & \text{perform } p_m \oplus B_1 \end{aligned} \tag{4}$$

where B_1 is the structuring element applied on the set P and C_Q is the boundary of set Q. A second case occurs when the border region of one set corresponds to the background of the other set. In this situation, we have erosions of the boundary elements

$$\begin{aligned} \text{If} \quad & p_m \in C_P \wedge q_m \in Q^c \\ \text{then} \quad & \text{perform } p_m \ominus B_1. \end{aligned} \tag{5}$$

No modifications are performed when both corresponding elements are members of their sets boundary

$$\begin{aligned} \text{If} \quad & p_m \in C_P \wedge q_m \in C_Q \\ \text{then} \quad & \text{perform no change.} \end{aligned} \tag{6}$$

The last situation corresponds to regions where the two sets coincide locally and no change is necessary, while (4) and (5) correspond to morphing transformations.

By including all these local changes, we define the following morphing transformation applied on the set P depending onto the set Q and on the structuring element B_1

$$\begin{aligned} & f(P|Q, B_1) \\ & \quad = \Big[(P \ominus B_1) \bigcup \Big(\Big(P \bigcap Q\Big) \oplus B_1\Big)\Big] \bigcap \Big(P \bigcup Q\Big). \end{aligned} \tag{7}$$

A similar morphing operation is defined onto the set Q depending on the set P and on the structuring element B_2

$$\begin{aligned} & f(Q|P, B_2) \\ & \quad = \Big[(Q \ominus B_2) \bigcup \Big(\Big(Q \bigcap P\Big) \oplus B_2\Big)\Big] \bigcap \Big(P \bigcup Q\Big). \end{aligned} \tag{8}$$

According to these transformations, the intersection of the two sets $P \cap Q$ is always retained by the morphing operations (4)–(6). One set will be eroded in those regions which correspond to the background of the other set while it will dilate in regions which correspond to the interior of the other set. The proposed morphing operation creates a new set which is a subset of $P \bigcup Q$.

In the proposed morphing algorithm, a particular situation occurs when the erosion of the first set includes the dilation of the second set

$$(P \ominus B_1) \supset (Q \oplus B_2). \tag{9}$$

We can easily observe that, in this case, (7) and (8) simplify to

$$f(P|Q, B_1) = P \ominus B_1 \tag{10}$$

$$f(Q|P, B_2) = Q \oplus B_2. \tag{11}$$

This situation is illustrated for 2-D sets in Fig. 1(a). On the other hand, we have the case when both P and Q contain subsets which are not included in the other set, i.e., $P - Q \neq \emptyset \wedge Q - P \neq \emptyset$. In this case, the operations defined by (7) and (8) are illustrated in Fig. 1(b).

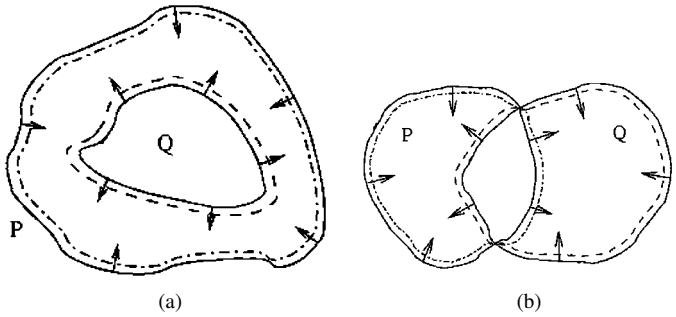

Fig. 1. Exemplification of mathematical morphology morphing. The result produced by (8) is represented with dashed lines while the result produced by (7) is represented with dot-dashed lines. Arrows denote dilation and erosion directions; (a) $(P \ominus B_1) \supset (Q \oplus B_2)$; (b) $P - Q \neq \varnothing$ and $Q - P \neq \varnothing$.

The result of the morphing operation applied on either set is a new set. These morphed sets are closer to each other in shape structure and size. In order to measure their similarity, we define a shape distance. Let us consider a structuring element $B(R)$ as a ball of radius R. Such a structuring element can be obtained from an elementary ball (ball of unit radius) after R successive dilations using the elementary ball as the structuring element. Let us define a shape distance between the original set and the morphed set as given by the size of the structuring element R. We conventionally assume a positive and a negative direction of morphing. After morphing the sets P and Q with the same structuring element $B(R)$, the distance of the morphed sets to their originating sets is

$$d(f(P|Q, B(R)), P) = -d(f(Q|P, B(R)), Q) = R \quad (12)$$

where the negative distance has been conventionally assigned. In the general case, this shape distance is not symmetrical

$$d(P, Q) \neq d(Q, P). \quad (13)$$

For isotropic interpolation, we use identical structuring elements, $B_1 = B_2 = B$, when morphing the two sets. In this case, each morphed set is equi-distant to its original set. The distance defined in (12) does not depend on the number of elements (pixels in a discretized 2-D space) eroded or added, but on the structural differences between the two shapes that are morphed and on the structuring element size. In the case when the elementary ball is used as structuring element, the shape distance between the original set and its morphing is one.

III. Geometrically Constrained Interpolation

The morphing operation defined by (7) and (8) is applied iteratively onto the sets resulted from the previous morphings. The succession of morphing operations creates new sets derived from the two initial extremes. With each iteration these sets are closer in shape and size to each other. Three-dimensional natural exemplifications of this morphological morphing approach can be found in tree rings and in crystal layer structures. By employing an alignment operation w, we can ensure that $P \bigcap Q \neq \varnothing$. The morphing interpolation is based on the following theorem.

Theorem 1: Always we can generate an intermediary set between two sets P and Q, satisfying $P \bigcap Q \neq \varnothing$, by iterating the set transformations defined in (7) and (8) onto their previous iteration output sets, until idempotency.

Proof: In order to prove the morphing interpolation convergence to idempotency, let us consider a set Y, representing the XOR operation for the two given sets

$$Y(Q, P) = XOR(Q, P) = \left(Q \bigcup P\right) - \left(Q \bigcap P\right). \quad (14)$$

We assume that the local morphing termination condition (6) does not occur at the next morphing iteration, which implies that

$$\left[\left(Q \bigcup P\right) \ominus B\right] \supset \left[\left(Q \bigcap P\right) \oplus B\right]. \quad (15)$$

In this case, we observe that by considering (7) and (8) and by grouping the resulting set components we obtain

$$\begin{aligned} &Y(f(P|Q), f(Q|P)) \\ &\quad = \left[f(P|Q) \bigcup f(Q|P)\right] - \left[f(P|Q) \bigcap f(Q|P)\right] \\ &\quad = \left[\left(\left(Q \bigcup P\right) \ominus B\right) - \left(\left(Q \bigcap P\right) \oplus B\right)\right] \bigcap \left(Q \bigcup P\right) \\ &\quad = Y(Q, P) \ominus B \end{aligned} \quad (16)$$

where for the sake of simplification we dropped out the dependency on the elementary structuring element from the expression of the morphing transformation. The morphing rules outlined in (4)–(6) are employed in the successive morphing operations. We can observe that erosion applies everywhere on the set Y, excepting for the points which fulfill the condition (6). Such points are not eroded. There is a clear interdependence between the set Y defined in (14) and the morphological shape distance defined in (12). While with each iteration the set Y is eroded as it is shown by (16), the distance between the resulting sets, morphed from P and Q, decreases correspondingly

$$\begin{aligned} &d(f(P|Q), f(Q|P)) \\ &\quad = d(P, Q) - d(f(P|Q), P) + d(f(Q|P), Q) \\ &\quad = d(P, Q) - 2 \end{aligned} \quad (17)$$

where we have considered an elementary structuring element. Let us denote the morphing at iteration t, initiated from the sets P and Q, by $f_t(P|Q)$ and $f_t(Q|P)$, respectively. As we have seen above, the morphing transformation corresponds to the conditional erosion of the set Y. According to the relationship (17), at each iteration the distance between the morphed sets decreases. Equation (6) represents a local stopping condition which is likely to extend with each iteration to a larger amount of elements from the boundary of the morphed sets. We can observe that this happens simultaneously with the shrinkage of the set Y which eventually becomes a closed contour. The interpolation termination condition corresponds to the case when we fulfill the morphing termination condition of (6) for all the boundary points of the two morphed sets. In this situation, the two morphed sets become idempotent. Let us assume that this

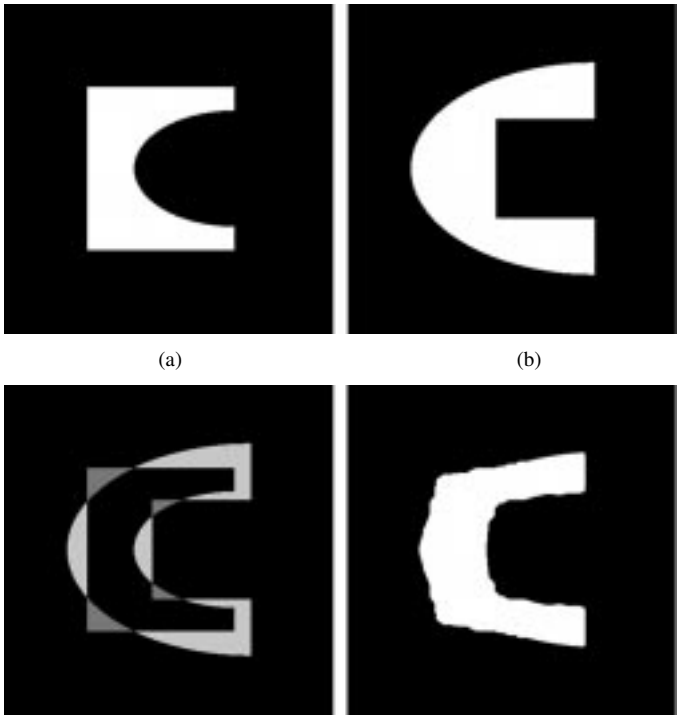

(a) (b) (c) (d)

Fig. 2. Shape-based interpolation of two sets. (a) fFirst set. (b) Second set. (c) Difference set. (d) Resulting interpolated set.

happens after t_1 iterations. Idempotency after t_1 iterations is shown by a zero distance between the resulting morphed sets

$$d(f_{t_1}(P|Q),\, f_{t_1}(Q|P)) = 0. \tag{18}$$

Let us denote by $\hat{M}$ the set obtained at the idempotency of the morphing transformation

$$\hat{M} = f_{t_1}(P|Q) = f_{t_1}(Q|P). \tag{19}$$

This set has similarities to both initial sets P and Q. The set $\hat{M}$ is equidistant, according to the distance measure defined in (12) to the original sets

$$d(P,\, \hat{M}) = -d(Q,\, \hat{M}). \tag{20}$$

The existence of a set which is equidistant to the initial sets and which corresponds to the case when the set Y becomes a contour proves the convergence of the morphing *Theorem* 1.

These results can be easily extended to discrete sets. Elements in such sets consists of hypervoxels in an n-dimensional space (pixels for 2-D sets). In order to exemplify this result, we consider the 2-D sets from Fig. 2(a) and (b). The initial difference set $Y(P, Q)$ is shown in Fig. 2(c). After five iterations ($t_1 = 5$) using the structuring element from Fig. 3, we get the interpolated set $\hat{M}$, displayed in Fig. 2(d). In this case, the distance between the interpolated set and the original sets is

$$d(P,\, \hat{M}) = -d(Q,\, \hat{M}) = 5 \tag{21}$$

which is equal to the number of morphing transformations performed by each of these sets until idempotency. The morphing in this example required mostly rectangular to circular shape transformations. We can observe that, despite certain discretization errors, the morphing transformations resulted in a good interpolation result. The interpolated set has similarities to both initial sets, shown in Fig. 2(a) and (b).

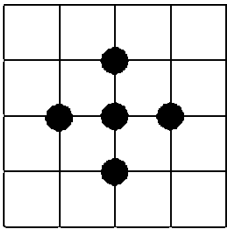

Fig. 3. Elementary ball structuring element.

All the above assumptions and derivations rely on the fact that we have identical structuring elements for morphing both sets P and Q. In this case, the resulting interpolated set is at equal distance to the given two sets according to (20). However, in certain situations, we may want to interpolate a set, which is at smaller distance to one or another of the given two sets, by using *a priori* knowledge. We can either use a larger structuring element for eroding/dilating the set which should be less similar to the interpolated set, or repeat the morphing for an additional number of times on that set using the same structuring element. In the case when considering discrete sets, these two approaches can provide slightly different results due to the discretization and approximation of the spherical structuring element on a discrete grid. Let us assume that we would like an interpolated set whose shape distance ratio to the initial sets is given by

$$\frac{|d(P, \hat{M}, B_1)|}{|d(Q, \hat{M}, B_2)|} = \frac{k_1}{k_2} \tag{22}$$

where we assume a structuring element B_1 for morphing P and B_2 for morphing Q. The ratio between the radii R_{B_1} and R_{B_2} of two hyper-spherical structuring elements, is given by

$$\frac{R_{B_1}}{R_{B_2}} = \frac{k_2}{k_1}. \tag{23}$$

Let us consider an ordered group of sets $P_0, P_1, \ldots, P_{N-1}$, representing cross-sections of a certain object, where N represents the total number of sets. The morphing procedure presented above interpolates a new group of sets between each two consecutive sets. In the general case, each new set is equi-distant to the original neighboring sets. The initial and the interpolated sets will form a new group of sets which can be used for a better visualization of the given 3-D object. We repeat the same procedure on the new pairs of consecutive sets for modeling the entire object to a finer detail. After K repetitions, the number of interpolated sets generated between two initial sets is $2^K - 1$. Evidently, there is an upper limit in the number of distinctly interpolated sets generated between two given consecutive sets. For N initial sets we obtain $(N-1)(2^K - 1)$ interpolated sets. The number of sets to be inserted depends on the relationship between the slice spacing and set element size. In the case of unequally spaced cross-section sets, a different number of sets must be interpolated between each two consecutive slices. Another way to deal with unequally spaced interpolation would be to generate all the possible intermediary sets

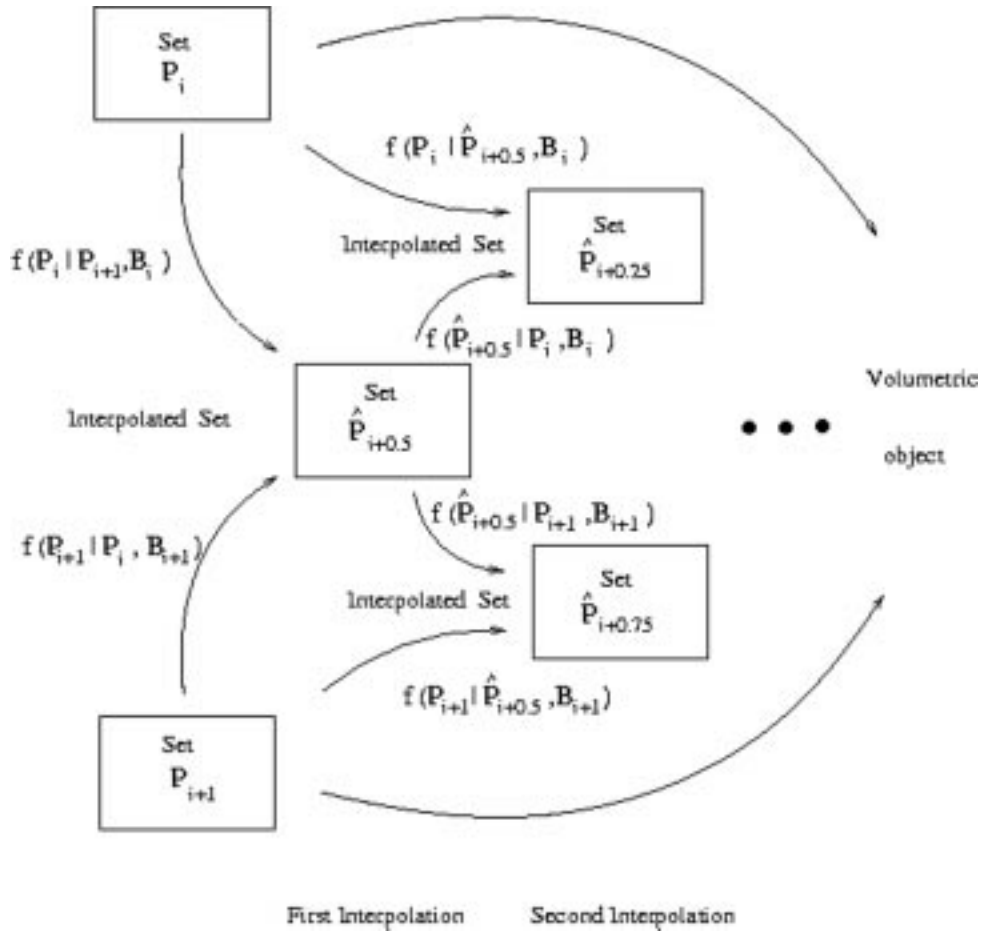

Fig. 4. Diagram describing the interpolation algorithm using morphing of consecutive set pairs.

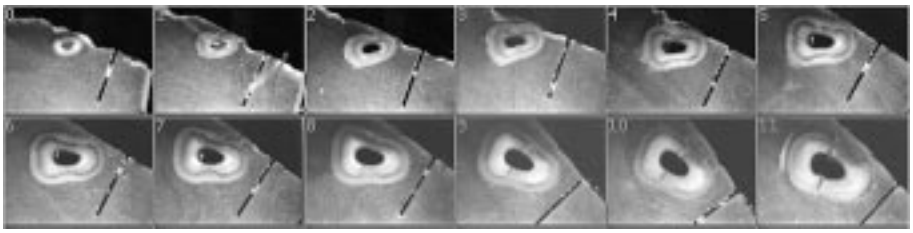

Fig. 5. Set of tooth slices in resin.

and to choose certain sets, according to their desired intraset distance. In this case, the number of interpolated sets is smaller than $(N-1)(2^K-1)$. The intermediate sets, denoted by $\hat{P}_{i+l/2^K}$ for $l = 1, \ldots, 2^K - 1$, represent an interpolation between the two initial sets P_i and P_{i+1}. Grey-level interpolation can be performed together with the shape interpolation [18]. The procedure of interpolation by successive morphing is exemplified in Fig. 4.

IV. Simulation Results

We have used the proposed morphological morphing interpolation algorithm for reconstructing the external and internal 3-D morphology of several teeth. Such an application is of interest in endodontology for representing tooth morphological structure [20]. The examples used in the experiments described in this paper represent normal tooth shapes that are reported in the dental literature. We reconstructed several tooth shapes using the proposed interpolation algorithm. Three examples are presented in this paper: an incisor (single root tooth); a premolar (two-root tooth); and a molar (three-root tooth). These teeth have been mechanically sliced and digitized. A set of incisor slices in resin is displayed in Fig. 5. The tooth borders as well as the root canal in each slice are segmented and the resulting slices are aligned using a semi-automatic procedure. Aligned slices are displayed in Fig. 6(a), for the incisor, in Fig. 6(b), for the premolar and in Fig. 6(c) for the molar, respectively. We have used the morphological interpolation algorithm described in Sections II and III in order to reconstruct the teeth from the given initial set of slices. In the case of the incisor, the morphing algorithm is applied iteratively four times. Thus we eventually produce $21 * (2^4 - 1) + 22 = 337$ slices from only 22 original slices. A set of interpolated frames from the incisor sequence is displayed in Fig. 7. We can observe from this

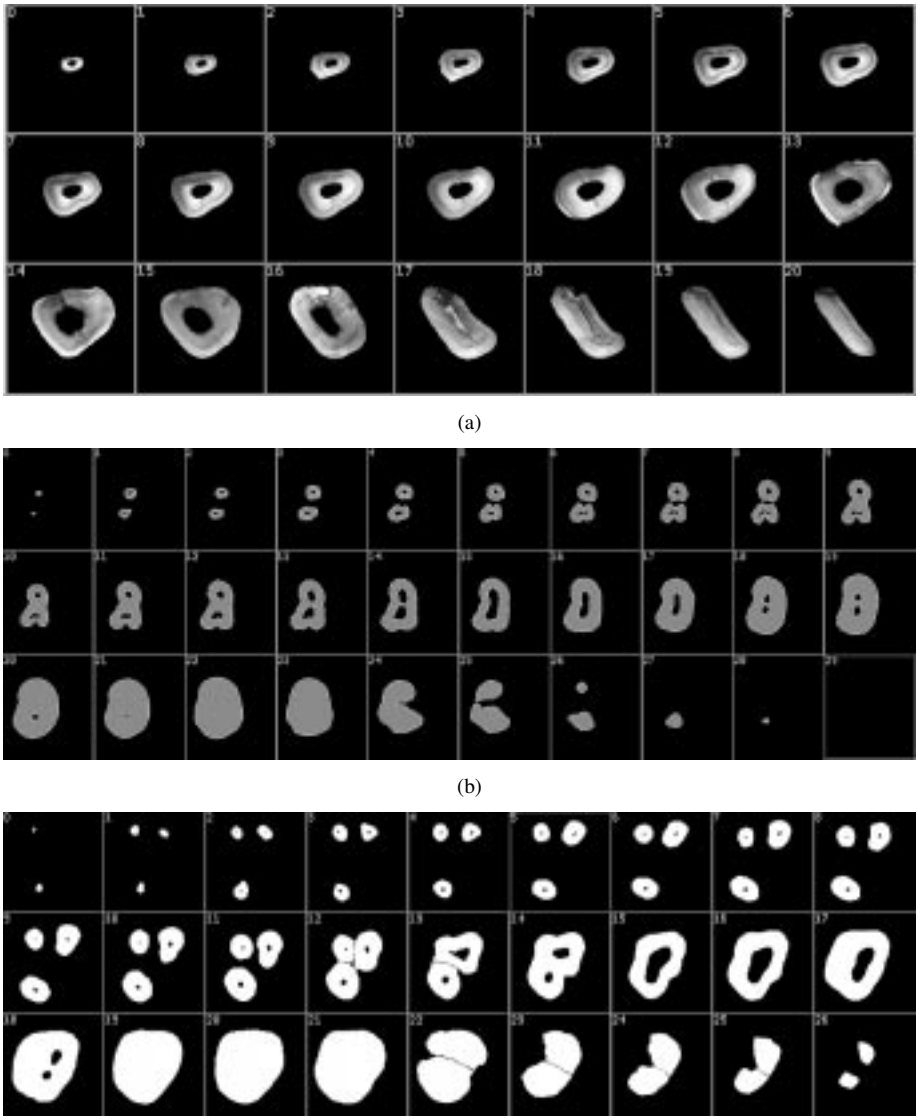

(a)

(b)

(c)

Fig. 6. Segmented and aligned tooth slice sets. (a) Incisor. (b) Premolar (two roots). (c) Molar (three roots).

figure that both canal and outer tooth surface are being smoothly changed from one slice to the next one. A grey-level interpolation algorithm [18] was used together with the proposed shape-based interpolation algorithm. This result shows a smooth transition even between slices having large geometrical variations in shape. Three-dimensional reconstructions from two different viewing angles are shown in Fig. 8(a) and (b) for the incisor, in Fig. 8(c) and (d) for the premolar, and in Fig. 8(e) and (f) for the molar, respectively. These volumes are reconstructed from the initial slices shown in Fig. 6. In all these figures, we can observe that the 3-D volumes are well reconstructed. The interpolation of the premolar and of the molar image sequences show the capability of morphing between slices with disconnected sets and those having compact sets. The morphology of the reconstructed teeth is quite accurate despite the fact that a large number of slices has been interpolated.

We have compared the mathematical morphological interpolation algorithm with a linear interpolation algorithm. The linear interpolation algorithm calculates line segments between pixels on object contours of the two slices, in both horizontal and vertical directions. The midpoints of these segments are considered as the interpolated slice contour by this algorithm. We have applied the linear interpolation algorithm on the incisor sequence displayed in Fig. 6(a). We employ a measure for assessing the performance provided by various interpolation algorithms in the following way. Let P_i, P_{i+1} and P_{i+2} be three original tooth slices and $\hat{P}_{i+1}$ be the result of interpolating P_i and P_{i+2}. Let $|P|$ denote set cardinality. The ratio $|Y(\hat{P}_{i+1}, P_{i+1})|/|P_{i+1}|$ representing the percentage of wrongly estimated pixels can be used as a performance measure. In Table I, we provide the results for reconstructing three different slices from the incisor group of sets as well as the average result for reconstructing any intermediary slice P_{i+1} from the given pair of sets P_i, P_{i+2} for any $i \in \{1, N-2\}$, where N is the number of initial sets. In order to assess the difference between original slices, we provide the normalized slice difference between the two slices used for interpolation. The case when using the tenth and the twelfth slices for estimating the eleventh slice is displayed in Fig. 9. The three consecutive slices are shown in Fig. 9(a)–(c), respectively. The interpolated slice by morphological morphing approach is

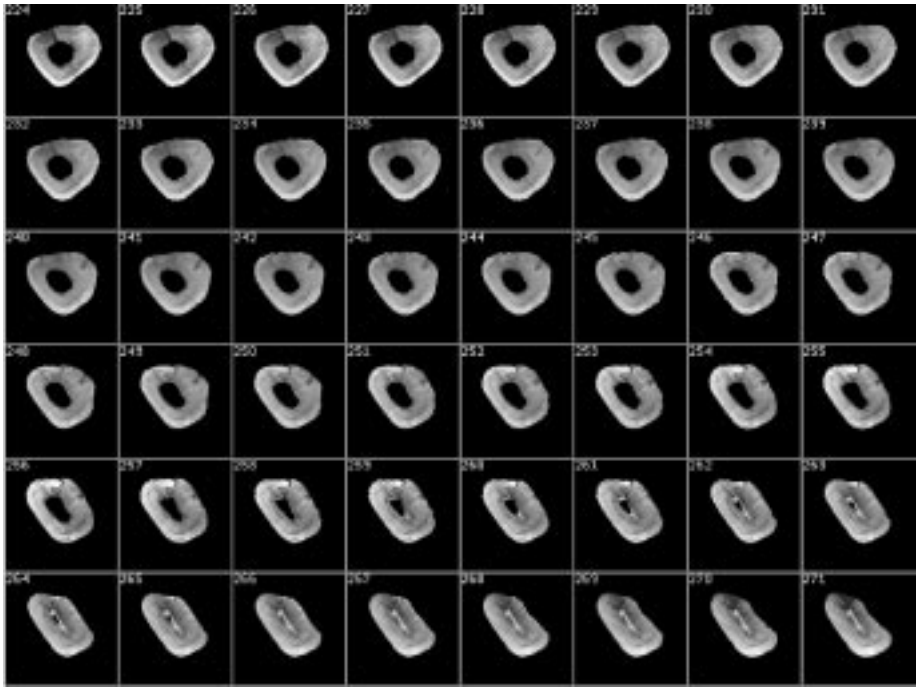

Fig. 7. Set of interpolated slices for an incisor.

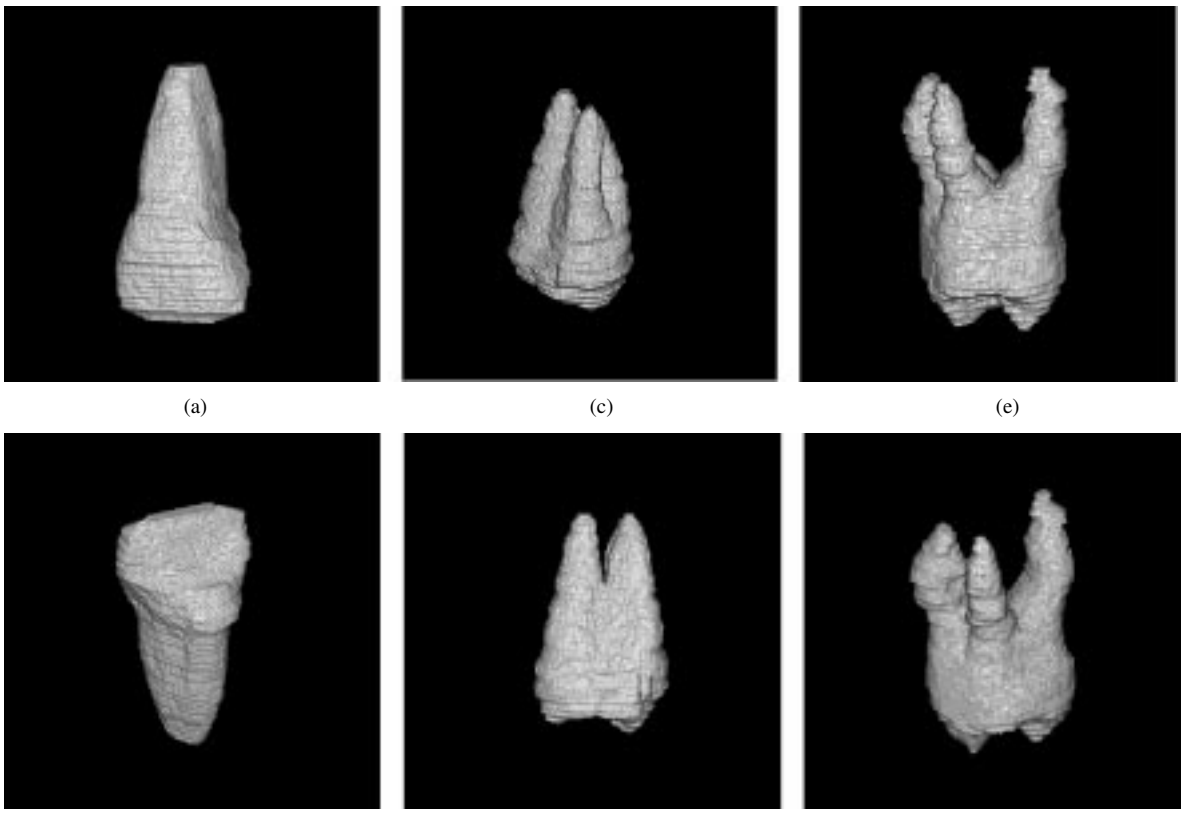

Fig. 8. Three-dimensional views of different reconstructed teeth. (a), (b) Incisor, (c), (d) Premolar. (e), (f) Molar.

displayed in Fig. 9(d), while in Fig. 9(f) we show the result provided by the linear interpolation approach. The difference between the interpolated and the original set are shown in Fig. 9(e) for the morphological morphing interpolation and in Fig. 9(g) for the linear interpolation. We can observe that the interpolated slice by morphing is more similar to the original slice than that interpolated by linear interpolation. The 3-D molar reconstructed by linear interpolation is displayed in Fig. 10(a), while in Fig. 10(b) we show the same molar reconstructed by morphological morphing as described in this paper. For comparison

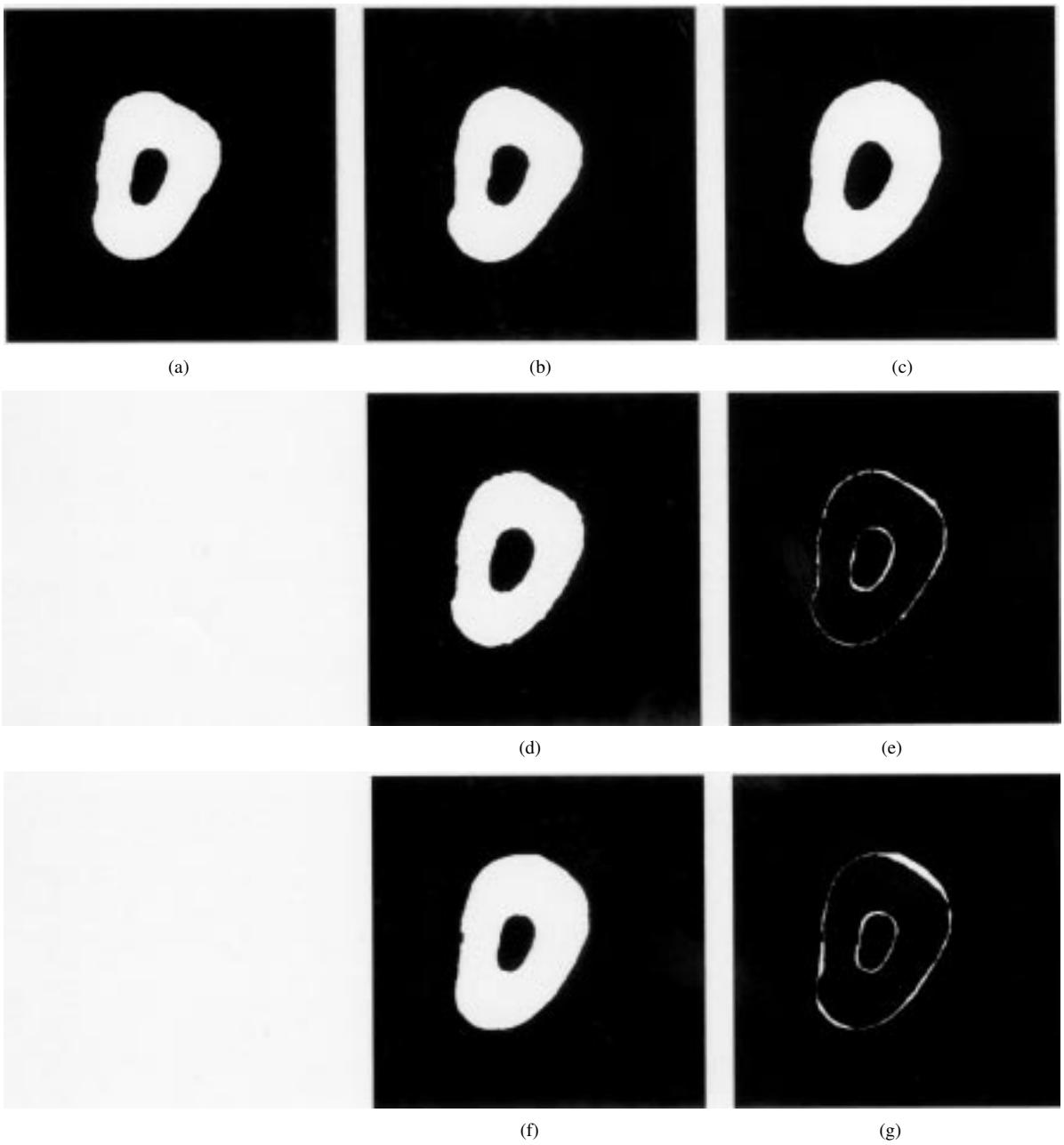

Fig. 9. Slices interpolated by morphological morphing and by linear interpolation from the tenth and twelfth slices of the incisor sequence compared with the real eleventh slice. (a) Tenth slice. (b) Eleventh slice. (c) Twelfth slice. (d) Morphological morphing. (e) Difference set. (f) Linear interpolation. (g) Difference set.

purposes both these volumes are visualized from the same view angle. We can observe that the shape of the molar is better reconstructed by the morphological morphing algorithm than by linear interpolation. These graphical results together with numerical results from Table I show that the proposed morphological morphing interpolation algorithm provides good experimental results in the case of 3-D tooth reconstruction from digitized slices.

V. Conclusion

In this paper, we propose a morphological morphing algorithm. We consider a group of sets representing sampled object cross sections at various depths. The proposed interpolation algorithm relies on a morphing transformation of each of two sets into the other one. The interpolated set is obtained for the idempotency of the morphed sets from neighboring slices under the proposed morphological transformation. This set has similarities in shape and size with both initial neighboring slices sets. The algorithm is iteratively repeated, by considering new pairs of neighboring slices, until generating an appropriate number of interpolated sets. After describing the algorithm we provide experimental results of its application for reconstructing the shape of various teeth from slices. The purpose of this algorithm is to create a database of various types of teeth. Such tooth volumes can be used for a virtual tooth drilling simulator in preclinical dentistry student training.

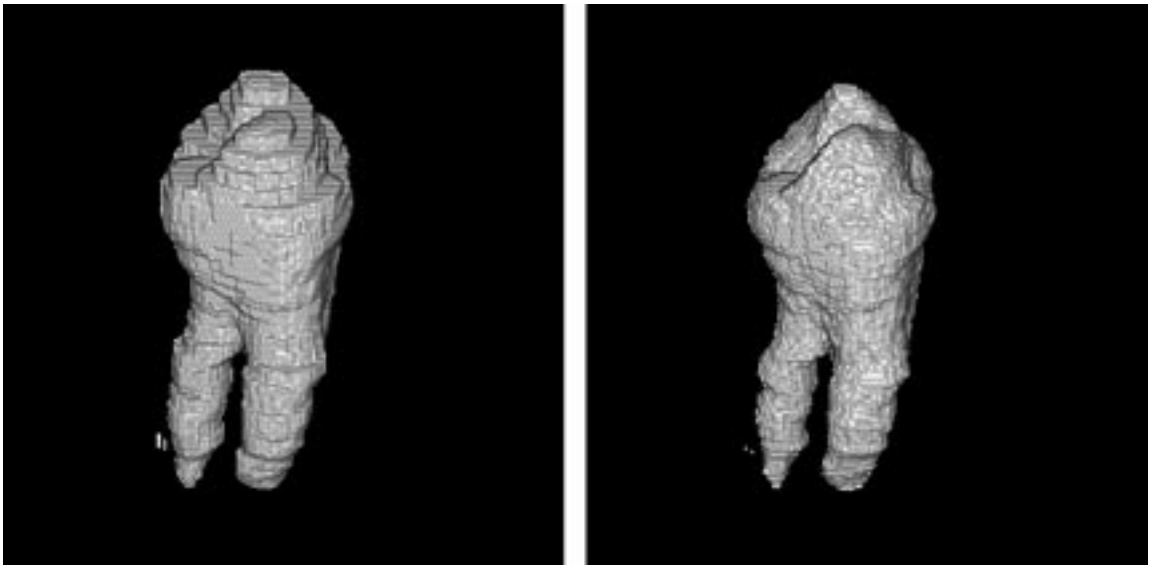

(a) (b)

Fig. 10. Reconstruction of a 3-D molar by (a) linear interpolation and (b) morphological morphing.

TABLE I
OBJECTIVE COMPARISON MEASURE BETWEEN MORPHOLOGICAL MORPHING AND LINEAR INTERPOLATION WHEN RECONSTRUCTING AN INCISOR

Frames i,i+1,i+2	Frame Difference (%) $\frac{\lvert Y(P_{i+2},P_i)\rvert}{\lvert P_i\rvert}$	Morphological Morphing (%) $\frac{\lvert Y(\dot{P}_{i+1},P_{i+1})\rvert}{\lvert P_{i+1}\rvert}$	Linear Interpolation (%) $\frac{\lvert Y(\dot{P}_{i+1},P_{i+1})\rvert}{\lvert P_{i+1}\rvert}$
4,5,6	62.9	5.9	11.925
10,11,12	26.8	6.84	9.46
18,19,20	27.2	7.5	14.28
Average results on the entire volume	51.5	9.25	11.46

REFERENCES

[1] G. Lohmann, *Volumetric Image Analysis: An Overview*. New York: Wiley-Teubner, 1998.

[2] A. Goshtasby, D. A. Turner, and L. V. Ackerman, "Matching of tomographic slices for interpolation," *IEEE Trans. Med. Imag.*, vol. 11, pp. 507–516, Dec. 1992.

[3] M. Moshfeghi, "Directional interpolation for magnetic resonance angiography data," *IEEE Trans. Med. Imag.*, vol. 12, pp. 366–379, June 1993.

[4] W. E. Higgins, C. J. Orlick, and B. E. Ledell, "Nonlinear filtering approach to 3-D grey-scale image interpolation," *IEEE Trans. Med. Imag.*, vol. 15, pp. 580–587, Aug. 1996.

[5] S. P. Raya and J. K. Udupa, "Shape-based interpolation of multidimensional objects," *IEEE Trans. Med. Imag.*, vol. 9, pp. 32–42, Feb. 1990.

[6] P. N. Werahera, G. J. Miller, G. D. Taylor, T. Brubaker, F. Daneshgari, and E. D. Crawford, "A 3-D reconstruction algorithm for interpolation and extrapolation of planar cross sectional data," *IEEE Trans. Med. Imag.*, vol. 14, pp. 765–771, Dec. 1995.

[7] G. T. Herman, J. Zheng, and C. A. Bucholtz, "Shape-based interpolation," *IEEE Computer Graphics and Applicat.*, vol. 12, pp. 69–79, May 1992.

[8] W. E. Higgins, C. Morice, and E. L. Ritman, "Shape-based interpolation of tree-like structures in three-dimensional images," *IEEE Trans. Med. Imag.*, vol. 12, pp. 439–450, Sept. 1993.

[9] S.-Y. Chen, W.-C. Lin, C.-C. Liang, and C.-T. Chen, "Improvement on dynamic elastic interpolation technique for reconstructing 3-D objects from serial cross sections," *IEEE Trans. Med. Imag.*, vol. 9, pp. 71–83, Feb. 1990.

[10] G. J. Grevera and J. K. Udupa, "An objective comparison of 3-D image interpolation methods," *IEEE Trans. Med. Imag.*, vol. 17, pp. 642–652, Apr. 1998.

[11] ——, "Shape-based interpolation of multidimensional grey-level images," *IEEE Trans. Med. Imag.*, vol. 15, pp. 881–892, June 1996.

[12] J. Serra, *Image Analysis and Mathematical Morphology*. New York: Academic, 1982.

[13] I. Pitas and A. N. Venetsanopoulos, *Nonlinear Digital Filters: Principles and Applications*. Norwell, MA: Kluwer Academic, 1990.

[14] M. Joliot and B. M. Mazoyer, "Three-dimensional segmentation and interpolation of magnetic resonance brain images," *IEEE Trans. Med. Imag.*, vol. 12, pp. 269–277, June 1993.

[15] B. Luo and E. R. Hancock, "Slice interpolation using the distance transform and morphing," in *Proc. Int.. Conf. Digital Signal Processing*, Santorini, Greece, 1997, pp. 1083–1086.

[16] V. Chatzis and I. Pitas, "Interpolation of 3-D binary images based on morphological skeletonization," *IEEE Trans. Med. Imag.*, vol. 19, pp. 699–710, July 2000.

[17] S. Beucher, "Sets, partitions and functions interpolations," in *Proc. Int. Symp. Mathematical Morphology and Its Applications to Image and Signal Processing IV*, Amsterdam, Netherlands, June 3–5, 1998, pp. 307–314.

[18] A. G. Borş, L. Kechagias, and I. Pitas, "Virtual drilling in 3-D objects reconstructed by shape-based interpolation," in *Lecture Notes in Computer Science*, C. Arcelli, L. P. Cordella, and G. Sanniti di Baja, Eds. Capri, Italy, May 2001, vol. 2059, Proc. Int. Workshop Visual Form, pp. 729–738.

[19] ——, "Shape-based interpolation using morphological morphing," in *Proc. IEEE Int. Conf. Image Processing*, vol. II, Thessaloniki, Greece, Oct. 7–10, 2001, pp. 161–164.

[20] K. Lyroudia, O. Pantelidou, G. Mikrogeorgis, N. Nikopoulos, and I. Pitas, "Three dimensional reconstruction: A new method for the evaluation of apical microleakage," *J. Endodont.*, vol. 26, no. 1, pp. 36–38, 2000.